

Development of high critical current density in multifilamentary round-wire $\text{Bi}_2\text{Sr}_2\text{CaCu}_2\text{O}_{8+\delta}$ by strong overdoping¹

T. Shen, J. Jiang, A. Yamamoto, U. P. Trociewitz, J. Schwartz, E.E. Hellstrom, and D.C. Larbalestier

Applied Superconductivity Center, National High Magnetic Field Laboratory, Florida State

University, Tallahassee, FL, 32310, USA

Abstract:

$\text{Bi}_2\text{Sr}_2\text{CaCu}_2\text{O}_{8+\delta}$ is the only cuprate superconductor that can be made into a round-wire conductor form with a high enough critical current density J_c for applications. Here we show that the $J_c(5\text{ T}, 4.2\text{ K})$ of such Ag-sheathed filamentary wires can be doubled to more than $1.4 \times 10^5\text{ A/cm}^2$ by low temperature oxygenation. Careful analysis shows that the improved performance is associated with a 12 K reduction in transition temperature T_c to 80 K and a significant enhancement in intergranular connectivity. In spite of the macroscopically untextured nature of the wire, overdoping is highly effective in producing high J_c values.

¹ To appear in Applied Physics Letters

Perhaps the most pressing wish of the large scale superconducting applications community is to develop a round wire multifilamentary conductor from a 100 K class superconductor, which could viably replace the two Nb-based materials, Nb-Ti and Nb₃Sn with T_c of 9 and 18 K, from which virtually all superconducting applications are presently made.¹ For more than 20 years the dream of using cuprate high temperature superconductors (HTS) with T_c in the 90 to 110 K range has fueled a conviction that helium-free magnets operating at much higher temperatures are possible. The three available HTS conductors all offer the possibility to generate magnetic fields far beyond the maximum of ~22 T possible with Nb₃Sn, since cuprates have critical fields at 4.2 K greater than 100 T, even in the inferior direction. But the major obstacle to their use is the tendency of cuprate grain boundaries (GBs) with misorientation angle $\theta > 3-4^\circ$ to have depressed J_c due to local GB suppression of the carrier density and the superconducting order parameter.^{2, 3} Thus (Bi,Pb)₂Sr₂Ca₂Cu₃O_x (Bi-2223) conductors have never achieved their full potential because only a partial uniaxial texture with FWHM ~10-12° can be developed,⁴ while coated conductors of YBa₂Cu₃O_{7- δ} (YBCO) show much higher J_c because a strong biaxial texture with FWHM < 5° can be developed by epitaxial or seeded growth.⁵⁻⁷ But large aspect ratio tapes, ~20:1 for Bi-2223 or typically 4000:1 for YBCO, are far from optimum, because it is hard to cable flat tape conductors and tapes have large hysteretic losses in perpendicular magnetic field **H**. Since the cuprate GB problem is widely believed to be intrinsic to their small carrier density and proximity to a parent, antiferromagnetic insulating state, understanding the remarkable properties of round-wire, Ag-sheathed Bi-2212 conductor has quite general importance. Unlike any other cuprate, Bi-2212 can attain high J_c in round wires which lack long-range texture. This letter addresses the final process step that greatly enhances their J_c and ties it to oxygenation treatments that overdope the Bi-2212 phase in ways that are generally not possible in Bi-2223 or YBCO.

Bi-2212 round wire is composed of a myriad of ~100-200 μm long and ~0.1-0.3 μm thick plate-like Bi-2212 grains, often arranged in 1-5 μm thick colonies that share a common *c*-axis with [001] twist boundaries⁸. Although the *c*-axis is often aligned perpendicular to the wire axis, there is no azimuthal texture. Despite this absence of long-range texture, powder-in-tube (PIT) Bi-2212 round

wire can carry remarkably high J_c values ($\sim 1 \times 10^5$ A/cm² at 45 T and 4.2 K)⁹. The combination of high J_c and poor texture suggests that GB transport in Bi-2212 round wire is much easier than in Bi-2223 and YBCO.

Partial-melt processing (see the typical multistep process in Fig. 1) is vital to develop high J_c .¹⁰ The conductor whose filament powder starts as essentially single-phase Bi-2212 is heated above the Bi-2212 peritectic temperature to melt the filaments, producing a liquid containing all elements including Ag, alkaline earth cuprate ((Sr,Ca)₁₄Cu₂₄O_x), and copper-free phase (Bi₉(Sr,Ca)₁₆O_x) mixture. Slow cooling, in this case 2.5 °C/hr, solidifies this mixture and below ~ 872 °C Bi-2212 grains nucleate. Much discussion on improving conductor J_c deals with manipulating the melt phase assemblages.¹¹ Here, we concentrate on the final portion of the heat treatment, which occurs after forming the Bi-2212 network, where we enhance the superconducting connectivity by slow cooling in an O₂-rich atmosphere.

We quenched 4 cm long sections of a Ag-sheathed wire containing 7 bundles of 85 Bi-2212 filaments fabricated by Oxford Superconducting Technology^{9, 12} at multiple points (Q836C means quenching from 836 °C) in the process using brine as the quench medium to preserve the high temperature microstructures and electromagnetic properties, without introducing damage that might reduce J_c .¹³ Thus we could directly correlate the superconducting properties to the high temperature state.

Microstructures were carefully examined and phase chemistry was determined using a field emission scanning electron microscope. The important point is that no observable change in the phase state occurred below the highest temperature examined here, 836 °C. T_c was evaluated from zero-field-cooled magnetic moments measured in a SQUID magnetometer on 5 mm long samples with the wire axis parallel to **H**. The irreversibility field H_{irr} was approximated by linear extrapolation of the Kramer function $\Delta M^{0.5} H^{0.25}$ to zero, defining H_K . ΔM is the hysteretic magnetization, which is proportional to J_c . 5 mm long samples were measured in a 14 T vibrating sample magnetometer with the wire axis perpendicular to **H** so that currents propagate along the wire axis across many GBs. The inter- and intra-grain contributions to the hysteretic moment ΔM were deduced from the remanent

moment $m_R(H_a)$, determined in the SQUID magnetometer by exposing sample to incrementally increasing magnetic field H_a followed by removal of the field and measurement of the remanent moment m_R . Magnetic flux first enters at weak regions such as GBs and finally into the grains, $m_R(H_a)$ in each case being given by the product of the screening currents I_c and the length scale of these currents.^{14, 15} Differentiation of $m_R(H_a)$ often shows two distinct peaks corresponding at low fields to *intergrain* currents circulating across GBs, while the higher-field peak corresponds to a combination of *intragrain* currents of high J_c and/or well connected current paths with long length scales. The transport J_c was determined at an electric field criterion of 10^{-6} V/cm with field perpendicular to the wire axis at 4.2 K using the Bi-2212 cross-section before reaction as the normalizing area.

Figure 1 compares the transport J_c at self field and 5 T at 4.2 K for each of the 3 quenched samples (836, 650, and 330 °C), together with a fully processed sample (FP) and the sample that was quenched from 836 °C and then given a final low temperature post-anneal (400 °C, 30 hr) in 1 bar flowing O₂ (Q836C+PA). We emphasize that there was no visible difference in the phase state and grain structure of these samples, since the Bi-2212 conversion process was complete at 855 °C, before any quenching. Fig. 1 shows that this slow cool at 170 °C/hr in 1 bar flowing O₂ from 836 °C dramatically enhanced J_c (4.2 K, 5 T) from 0.7 to 1.4×10^5 A/cm². Self field and 5 T J_c are raised similarly.

Figure 2 shows that as the quench temperature decreases, the transition loses its onset kink and T_c monotonically decreases from ~92 K (836 °C) to ~83 K (< 480 °C), indicating strong oxygen pickup, since T_c of cuprates is a parabolic function of hole concentration that increases with oxygen content δ in Bi₂Sr₂CaCu₂O_{8+ δ} .¹⁶ δ strongly depends on temperature, increasing from 0.2 at 830 °C to 0.25 at 300 °C in 1 bar oxygen.¹⁶ However, all transitions are broad, partly due to small filament dimensions (~20 μ m), as well perhaps due to residual compositional inhomogeneities, preferential flux penetration at high-angle grain boundaries, Bi₂(Sr,Ca)₂CuO_x (Bi-2201) intergrowths, or other secondary phases, and voids. The Q836C+PA sample has the lowest T_c with an onset of 80 K, indicating that it has the highest oxygen concentration.

Figure 3 plots $H_K(T)$ which exhibits the usual behavior of $H_{irr}(T)$, increasing steeply around 20 K.¹⁷ At 20 K, $H_{irr}(T)$ increased from ~ 5.6 T for Q836C to 7.4 T for fully processed wire, while the Q836C+PA sample shows the highest $H_K(20\text{ K})$ of 8.1 T. This enhancement is explained by a reduced intra-grain electronic anisotropy brought on by the increased carrier density of the overdoped state.^{18,}

19

Figure 4 shows that the remanent current flow paths produce two well separated peaks in $dm_R/d\log H_a$. It is striking that low temperature oxygenation preferentially enhances the first peak in which intergrain paths dominate. The clear implication is that the long-range current flow across GBs is enhanced by oxygenation.

Our central result is that low temperature oxygenation of a macroscopically untextured, round-wire multifilamentary Bi-2212 conductor produces a more than 2 fold enhancement of the in-field J_c (Fig. 1). These treatments enable the high J_c values needed for very-high-field magnets, as demonstrated by the generation of 2.5 T in a 20 T background field²⁰ and 1 T in a 31 T background field²¹, 32 T being a field more than 50% higher than can be generated with any Nb-based magnet. This oxygen pick up overdopes the Bi-2212 phase, decreasing T_c from 92 to 80 K (Fig. 2), but in all other respects enhancing the superconducting properties (Figs. 1-4). Especially valuable to J_c may be the connectivity enhancement shown in Fig. 4.

The mechanisms of decreased current transport through planar cuprate GBs have been extensively studied.^{2,3,5} Cuprate GBs develop an increasingly suppressed superconducting order parameter (OP) and J_c as θ increases.³ This OP suppression is amplified by the extra ionic charge, band bending, and strain-driven O_2 depletion in the vicinity of the GB, all of which lead to the GB being underdoped with respect to the grains and closer to the parent non-superconducting state. Neither Bi-2223 nor YBCO can be more than lightly overdoped, thus their GBs are underdoped. The benefits of overdoped GBs are seen in the properties of Ca-doped YBCO, because Ca does allow carrier overdoping of the GB²²⁻²⁴, and also in some bulk Bi-2212 bicrystal studies²⁵. The striking present result is that overdoping an untextured Bi-2212 wire makes a hugely positive influence on J_c . The poorly oxygenated Q836C and Q650C wires show a characteristic shoulder at 60-82 K in the $m(T)$

curves (Fig. 2), suggesting a decreased T_c at hole-deficient Bi-2212 grain boundaries. Lower-temperature oxygenation removes this shoulder and sharpens the T_c transition, while reducing the T_c onset. We emphasize that the resulting J_c values of 10^5 A/cm² or more are practical values that now enable the next generation of very high field magnets,^{20, 21} which makes this overdoping route to a round wire conductor of great practical and scientific interest.

This work was supported by U. S. National Science Foundation Division of Material Research through DMR-0654118 and the State of Florida. The authors are grateful to Van S. Griffin, Natanette C. Craig, and Bill Starch for technical assistance.

References

- ¹R. M. Scanlan, A. P. Malozemoff and D. C. Larbalestier, Proceedings of The IEEE **92**, 1639-1654 (2004).
- ²H. Hilgenkamp and J. Mannhart, Reviews of Modern Physics **74**, 485 (2002).
- ³A. Gurevich and E. A. Pashitskii, Phys. Rev. B **57**, 13878 (1998).
- ⁴N. Ayai, S. Kobayashi, M. Kikuchi, T. Ishida, J. Fujikami, K. Yamazaki, S. Yamade, K. Tatamidani, K. Hayashi, K. Sato, H. Kitaguchi, H. Kumakura, K. Osamura, J. Shimoyama, H. Kamijyo and Y. Fukumoto, Physica C **468**, 1747-1752 (2008).
- ⁵D. Larbalestier, A. Gurevich, D. M. Feldmann and A. Polyanskii, Nature **414**, 368-377 (2001).
- ⁶S. R. Foltyn, L. Civale, J. L. MacManus-Driscoll, Q. X. Jia, B. Maiorov, H. Wang and M. Maley, Nat. Mater. **6**, 631-642 (2007).
- ⁷J. Gutierrez, A. Llordes, J. Gazquez, M. Gibert, N. Roma, S. Ricart, A. Pomar, F. Sandiumenge, N. Mestres, T. Puig and X. Obradors, Nat. Mater. **6**, 367-373 (2007).
- ⁸Y. Feng, K. E. Hautanen, Y. E. High, D. C. Larbalestier, R. Ray, E. E. Hellstrom and S. E. Babcock, Physica C **192**, 293-305 (1992).
- ⁹H. P. Miao, K. R. Marken, M. Meinesz, B. Czabaj and H. Seung, IEEE Trans. Appl. Supercon. **15**, 2554-2557 (2005).

- ¹⁰K. Heine, J. Tenbrink and M. Thoner, *Appl. Phys. Lett.* **55**, 2441-2443 (1989).
- ¹¹H. Kumakura, H. Kitaguchi, K. Togano and N. Sugiyama, *J. Appl. Phys.* **80**, 5162-5168 (1996).
- ¹²K. R. Marken, H. Miao, M. Meinesz, B. Czabaj and S. Hong, *IEEE Trans. Appl. Supercon.* **13**, 3335-3338 (2003).
- ¹³T. Shen, E. E. Hellstrom, J. Jiang, D. C. Larbalestier and J. Schwartz, submitted to *Supercon. Sci. Technol.*, September, 2009.
- ¹⁴K. H. Müller, C. Andrikidis, H. K. Liu and S. X. Dou, *Phys. Rev. B* **50**, 10218 (1994).
- ¹⁵A. Yamamoto, A. A. Polyanskii, J. Jiang, F. Kametani, C. Tarantini, F. Hunte, J. Jaroszynski, E. E. Hellstrom, P. J. Lee, A. Gurevich, D. C. Larbalestier, Z. A. Ren, J. Yang, X. L. Dong, W. Lu and Z. X. Zhao, *Supercon. Sci. Technol.* **21**, 095008 (2008).
- ¹⁶P. Majewski, *Adv. Mater.* **6** (6), 460-469 (1994).
- ¹⁷B. Chen, W. P. Halperin, P. Guptasarma, D. G. Hinks, V. F. Mitrovic, A. P. Reyes and P. L. Kuhns, *Nat. Phys.* **3** (4), 239-242 (2007).
- ¹⁸K. Kishio, J. Shimoyama, T. Kimura, Y. Kotaka, K. Kitazawa, K. Yamafuji, Q. Li and M. Suenaga, *Physica C* **235-240**, 2775-2776 (1994).
- ¹⁹J. Shimoyama, Y. Nakayama, K. Kitazawa, K. Kishio, Z. Hiroi, I. Chong and M. Takano, *Physica C* **281**, 69-75 (1997).
- ²⁰H. Miao, M. Meinesz, Y. Huang, B. Czabaj, J. Parrell and S. Hong, presented at the International Conference on Cryogenic Materials, Tucson, AZ, 2009.
- ²¹U. P. Trociewitz, private communication (July 12, 2009).
- ²²A. Schmehl, B. Goetz, R. R. Schulz, C. W. Schneider, H. Bielefeldt, H. Hilgenkamp and J. Mannhart, *Europhys. Lett.* **47**, 110-115 (1999).
- ²³G. Hammerl, A. Schmehl, R. R. Schulz, B. Goetz, H. Bielefeldt, C. W. Schneider, H. Hilgenkamp, J. Mannhart, *Nature* **407**, 162-164 (2000).
- ²⁴G. A. Daniels, A. Gurevich and D. C. Larbalestier, *Appl. Phys. Lett.* **77**, 3251-3253 (2000).
- ²⁵J. Wang, I. Tsu, X. Y. Cai, R. J. Kelley, M. D. Vaudin, S. E. Babcock and D. C. Larbalestier, *J. Mat. Res.* **11**, 868-877 (1996).

Figure Captions:

Fig.1 (Color online) Significant increases occur in the self field and 5 T, 4.2 K transport J_c of Bi-2212 round wire in the final stage of the partial-melt process (inset). In flowing 1 bar O_2 , samples were melted at a maximum temperature of 894 °C and slowly cooled at 2.5 °C/hr to 836 °C, where they were annealed for 48 hr before being cooled at 170 °C/hr to room temperature. Samples were quenched at 836 °C, 650 °C, and 330 °C. A fully-processed (FP) wire and an oxygen-rich sample, which was quenched at 836 °C then post annealed at 400 °C for 30 hr in 1 bar flowing O_2 , are also shown. These samples are referred to Q836C, Q650C, Q330C, FP, and Q836C+PA. The dashed lines are given to guide the eye.

Figure 2 (Color online) Zero-field-cooled magnetic moments of Ag-sheathed Bi-2212 multifilament round wire Q836C, Q650C, Q330C, FP, and Q836C+PA induced by warming in a field of 1 mT applied parallel to the wire axis, indicates that significant oxygen overdoping occurs during the final cooling to room temperature.

Figure 3 (Color online) Kramer irreversibility field as a function of temperature for Q836C, Q650C, Q330C, FP, and Q836C+PA. Inset shows our method of determining H_K .

Figure 4 (Color online) Dependence of the remanent magnetic moment m_R (inset) and its derivative for the Bi-2212 round wires as measured for increasing fields applied parallel to the wire axis at 5 K. Note that the greatest connectivity is shown by sample Q836C+PA.

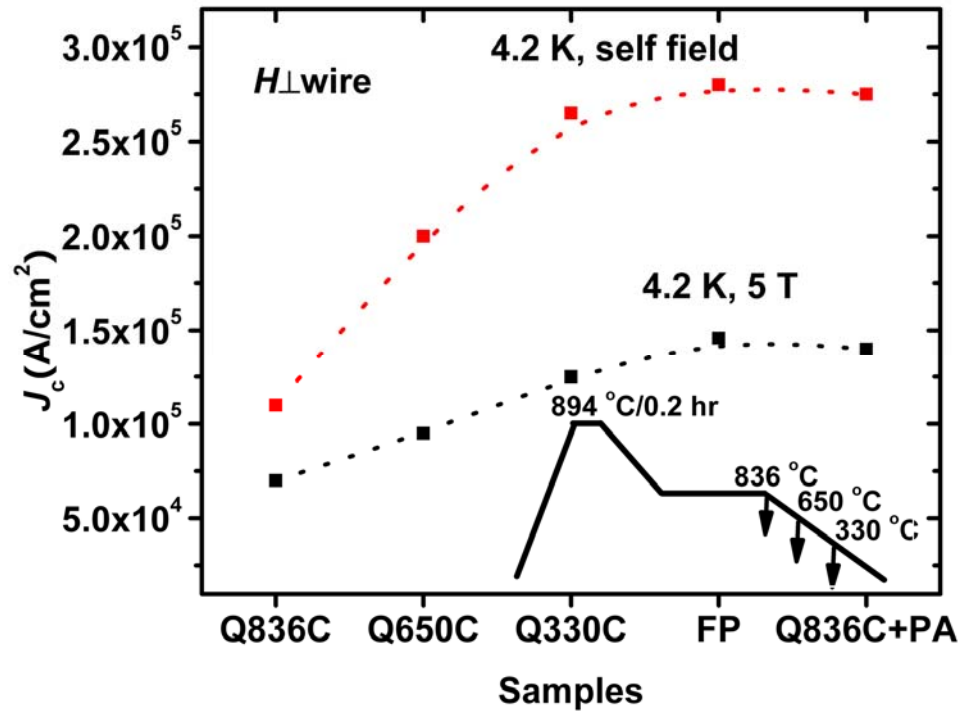


Figure 1

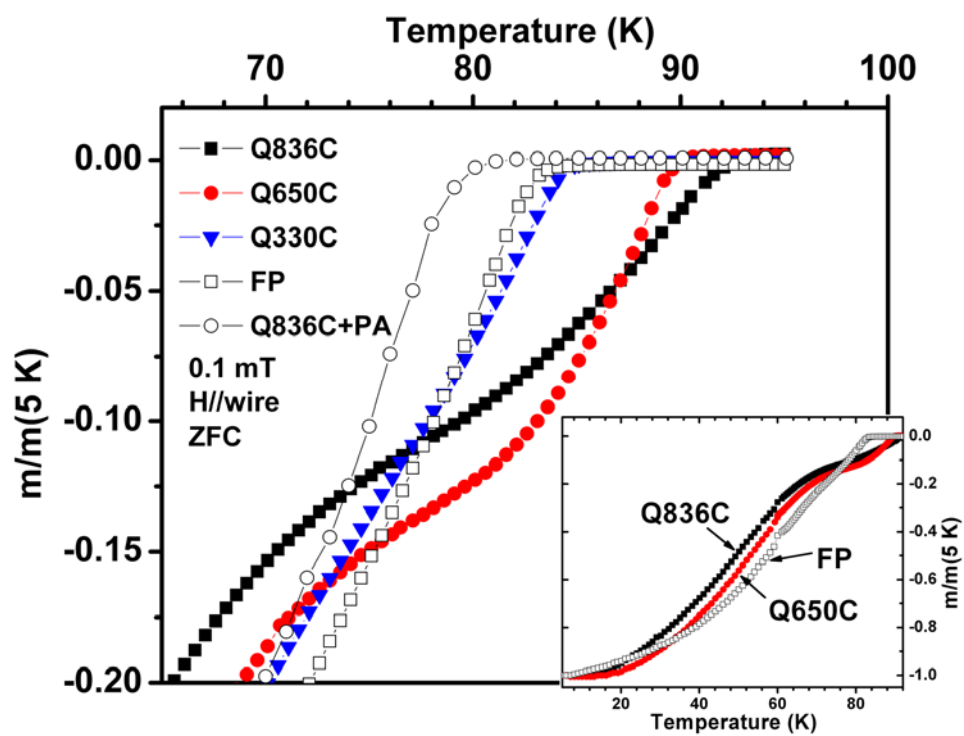


Figure 2

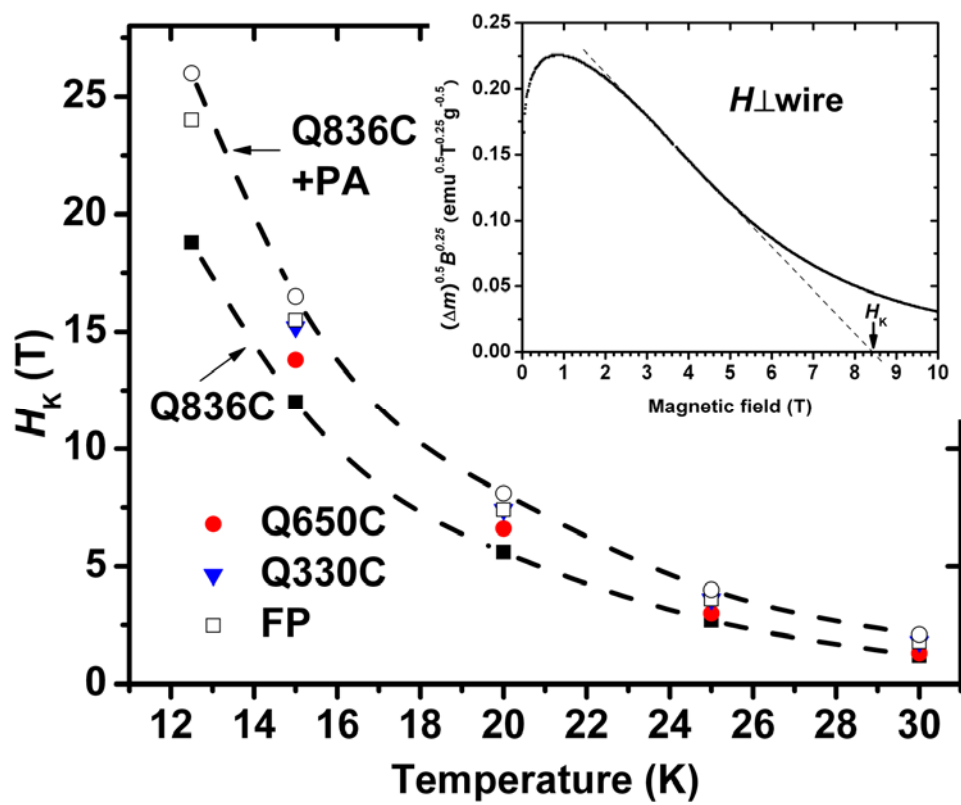


Figure 3

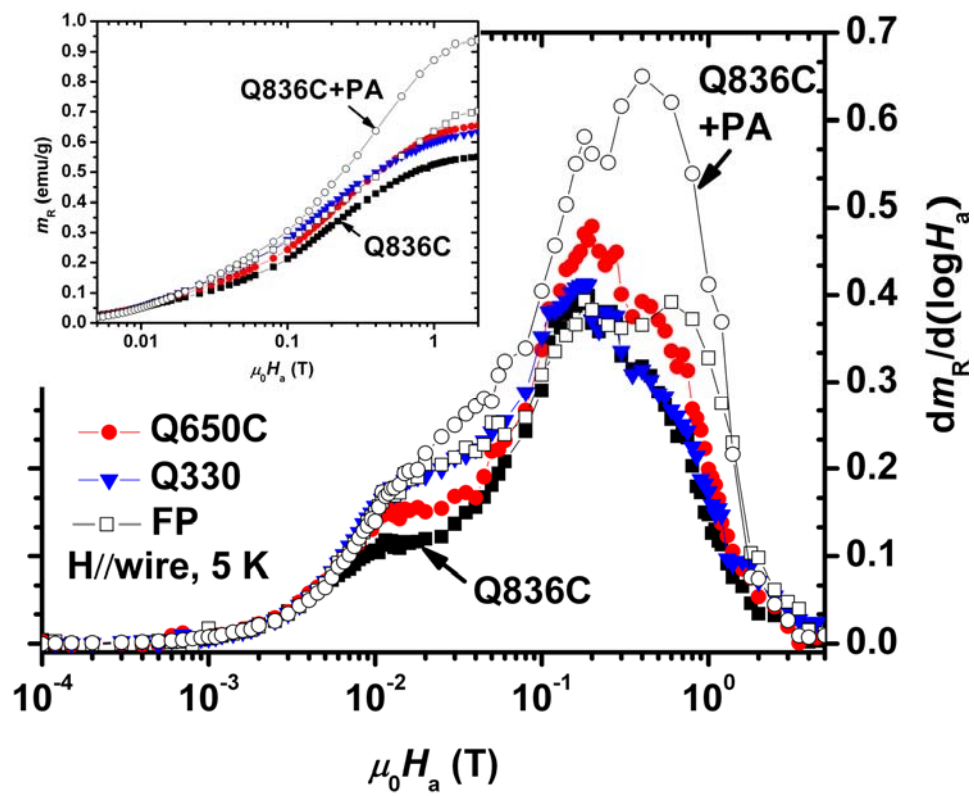


Figure 4